

Instituto de Física
Universidade de São Paulo

**Radion and Higgs Signals in Peripheral Heavy Ion Collisions
at the LHC**

S.M. Lietti¹ and C.G. Roldão²

*1. Instituto de Física, Universidade de São Paulo, C.P. 66318, 05315-970,
SP, Brasil*

*2. Instituto de Física Teórica, Universidade Estadual Paulista, Rua
Pamplona 145, CEP1405-900, SP, Brasil*

Publicação IF - 1548/2002



THE UNIVERSITY OF CHICAGO

PHILOSOPHY DEPARTMENT

PHILOSOPHY 301

PHILOSOPHY 302

PHILOSOPHY 303

PHILOSOPHY 304

PHILOSOPHY 305

PHILOSOPHY 306

PHILOSOPHY 307

PHILOSOPHY 308

PHILOSOPHY 309

PHILOSOPHY 310

PHILOSOPHY 311

PHILOSOPHY 312

PHILOSOPHY 313

PHILOSOPHY 314

PHILOSOPHY 315

PHILOSOPHY 316

PHILOSOPHY 317

PHILOSOPHY 318

PHILOSOPHY 319

PHILOSOPHY 320

Radion and Higgs Signals in Peripheral Heavy Ion Collisions at the LHC.

S. M. Lietti¹ and C. G. Roldão²

¹*Instituto de Física da USP,*

C.P. 66.318, São Paulo, SP 05389-970, Brazil.

²*Instituto de Física Teórica, Universidade Estadual Paulista,*

Rua Pamplona 145, CEP 01405-900 São Paulo, Brazil.

(May 22, 2002)

Abstract

We investigate the sensitivity of the heavy ion mode of the LHC to Higgs boson and Radion production via photon-photon fusion through the analysis of the processes $\gamma\gamma \rightarrow \gamma\gamma$, $\gamma\gamma \rightarrow b\bar{b}$, and $\gamma\gamma \rightarrow gg$ in peripheral heavy ion collisions. We suggest cuts to improve the Higgs and Radion signal over standard model background ratio and determine the capability of LHC to detect these particles production.

I. INTRODUCTION

The standard model (SM) has been very successful in accounting for almost all experimental data. The Higgs boson is the only particle in the SM that has not yet been confirmed experimentally. It is responsible for the mass generation of fermions and gauge bosons. The search for the Higgs boson is the main priority in high energy experiments and hints of its existence may have been already seen at LEP [1] at around $m_H \sim 115$ GeV. Nevertheless, the SM can only be a low energy limit of a more fundamental theory because it cannot explain a number of theoretical issues, one of which is the gauge hierarchy problem between the only two known scales in particle physics – the weak and Planck scales. Recent advances in string theories have revolutionized our perspectives and understanding of the problems, namely, the Planck, grand unification, and string scales can be brought down to a TeV range with the help of extra dimensions, compactified or not. Arkani-Hamed *et al.* [2] proposed that using compactified dimensions of large size (as large as mm) can bring the Planck scale down to TeV range. Randall and Sundrum [3] proposed a 5-dimensional space-time model with a nonfactorizable metric to solve the hierarchy problem. The Randall-Sundrum model (RSM) has a four-dimensional massless scalar, the modulus or Radion. The most important ingredients of the above model are the required size of the Radion field such that it generates the desired weak scale from the scale M (\approx Planck scale) and the stabilization of the Radion field at this value. A stabilization mechanism was proposed by Goldberger and Wise [4].

$$\frac{dL}{d\tau} = \int_{\tau}^1 \frac{dx}{x} F(x) F(\tau/x), \quad (6)$$

where $\tau = \hat{s}/s$, \hat{s} is the square of the center of mass (c.m.s.) system energy of the two photons and s of the ion-ion system. The total cross section $AA \rightarrow AA\gamma\gamma \rightarrow AAX$, where X are the particles produced by the $\gamma\gamma$ process, is

$$\sigma(s) = \int d\tau \frac{dL}{d\tau} \hat{\sigma}(\hat{s}), \quad (7)$$

where $\hat{\sigma}(\hat{s})$ is the cross-section of the subprocess $\gamma\gamma \rightarrow X$.

We choose to use the conservative and more realistic photon distribution of Cahn and Jackson [10], including a prescription proposed by Baur [8] for realistic peripheral collisions, where we must enforce that the minimum impact parameter (b_{min}) should be larger than $R_1 + R_2$, where R_i is the nuclear radius of the ion i . A useful fit for the two-photon luminosity is:

$$\frac{dL}{d\tau} = \left(\frac{Z^2 \alpha}{\pi} \right)^2 \frac{16}{3\tau} \xi(z), \quad (8)$$

where $z = 2MR\sqrt{\tau}$, M is the nucleus mass, R its radius and $\xi(z)$ is given by

$$\xi(z) = \sum_{i=1}^3 A_i e^{-b_i z}, \quad (9)$$

which is a fit resulting from the numerical integration of the photon distribution, accurate to 2% or better for $0.05 < z < 5.0$, and where $A_1 = 1.909$, $A_2 = 12.35$, $A_3 = 46.28$, $b_1 = 2.566$, $b_2 = 4.948$, and $b_3 = 15.21$. For $z < 0.05$ we use the expression (see Ref. [10])

$$\frac{dL}{d\tau} = \left(\frac{Z^2 \alpha}{\pi} \right)^2 \frac{16}{3\tau} \left[\ln \left(\frac{1.234}{z} \right) \right]^3. \quad (10)$$

In this paper we consider electromagnetic processes of peripheral Ar-Ar and Pb-Pb collisions in order to produce a Higgs and/or Radion scalar via photon-photon fusion since the pomeron contributions are negligible for subprocesses with center of mass energy close to the Higgs mass. According to Ref. [14], the total center of mass energy for $^{40}_{18}\text{Ar}$ ($^{208}_{82}\text{Pb}$) is equal to 7 (5.5) TeV/nucleon and an average luminosity of 5.2×10^{29} (4.2×10^{26}) $\text{cm}^{-2} \text{s}^{-1}$, which implies an effective photon-photon luminosity for $m_{\gamma\gamma} = 115$ GeV equals to 2×10^{28} (8×10^{26}) $\text{cm}^{-2} \text{s}^{-1}$ [0.63 (0.0025) pbarn $^{-1}$ year $^{-1}$] at LHC, as can be seen in Figure 1, which was extracted from Ref. [14]. We will also consider the optimistic possibility of Ca-Ca collisions [15,16], where the total center of mass energy for $^{40}_{20}\text{Ca}$ is equal to 7 TeV/nucleon and an average luminosity of 5×10^{30} $\text{cm}^{-2} \text{s}^{-1}$, which implies an effective photon-photon luminosity for $m_{\gamma\gamma} = 115$ GeV equals to 1.92×10^{29} $\text{cm}^{-2} \text{s}^{-1}$ (6 pbarn $^{-1}$ year $^{-1}$).

IV. RESULTS

In our analyses, we computed the cross sections for the Higgs and Radion production via photon-photon fusion in peripheral heavy ion collisions at LHC, with the subsequent decay

of the Higgs and/or Radion into $\gamma\gamma$, $b\bar{b}$ and gg pairs. The main sources of background for these processes are the box diagram for the process $\gamma\gamma \rightarrow \gamma\gamma$, the usual electromagnetic tree level diagrams for the process $\gamma\gamma \rightarrow b\bar{b}$, and the box diagram $\gamma\gamma \rightarrow gg$ and the usual tree level diagrams $\gamma\gamma \rightarrow q\bar{q}$, where $q = u, d, s, c$, for the process $\gamma\gamma \rightarrow gg$.

We begin our analyses using similar cuts and efficiencies as the ones ATLAS Collaboration [17] applied in their studies of Higgs boson searches. Our initial results are obtained imposing the following acceptance set of cuts:

$$p_T^{\gamma(b)[g]} > 25 \text{ GeV} \quad , \quad |\eta_{\gamma(b)[g]}| < 2.5 \quad , \quad \Delta R_{\gamma\gamma(bb)[gg]} > 0.4 \quad , \quad (11)$$

and taking into account an efficiency for reconstruction and identification of one photon of 84%, an efficiency of reconstruction for $H \rightarrow b\bar{b}$ of 90% with a b-tagging of 60% per each quark b [17], and finally an efficiency of reconstruction for $H \rightarrow q\bar{q}$ or gg of 80%. Taking all these efficiencies into account, the cross sections are evaluated with a total efficiency factor of 70(32)[80]% for the decay H or $R \rightarrow \gamma\gamma(bb)[gg]$. The results are presented in Table I for a Higgs and Radion masses of 115 GeV, with $\Lambda_R = 4v \approx 1$ TeV, in peripheral Ar-Ar and Pb-Pb collisions at LHC. Results for Ca-Ca collisions at LHC can also be obtained, according to Equation (8), by simply multiplying the results for Ar-Ar collisions by the factor $(\frac{Z_{Ca}}{Z_{Ar}})^4 = (\frac{20}{18})^4 \approx 1.524$.

In order to improve the Higgs and Radion signal over SM background, i.e., all other Feynman diagrams that contribute to the process considered, we have studied several kinematical distributions of the final state particles. Since the Higgs and Radion interactions occur mainly when these particles are produced on-shell, the most promising one is the invariant mass of the final particles.

The behavior of the normalized invariant mass distribution of the final state particles is plotted in Figure 2 for the process $\gamma\gamma \rightarrow b\bar{b}$ with a Higgs mass and a Radion mass equal to 115 GeV and $\lambda_R = 4v \approx 1$ TeV. For instance, if we impose an additional cut of $|m_{b\bar{b}} - m_H| < 15$ GeV in the process $\gamma\gamma \rightarrow b\bar{b}$, the value for the SM background cross section in peripheral Ar-Ar collisions is reduced from 6.927 pb to 0.8486 pb, while the value for the Higgs (Radion) cross section ($\gamma\gamma \rightarrow H(R) \rightarrow b\bar{b}$) is almost unaffected, varying from 0.1038(1.923 $\times 10^{-2}$) pb to 0.1038(1.919 $\times 10^{-2}$) pb when the invariant mass cut is imposed. Similar behavior is observed in the processes $\gamma\gamma \rightarrow \gamma\gamma$ and $\gamma\gamma \rightarrow gg$, as can be seen in Table II. Therefore we collected final states $\gamma\gamma$, $b\bar{b}$ and gg events whose invariant masses fall in bins of size of 30 GeV around the Higgs (Radion) mass

$$m_{H(R)} - 15 \text{ GeV} < m_{\gamma\gamma(bb)[gg]} < m_{H(R)} + 15 \text{ GeV} \quad (12)$$

in order to evaluate our results.

Considering the effective photon-photon luminosities given by Figure 1 and Refs. [14,15], we note that the Ar-Ar(Ca-Ca) luminosity is $\approx 250(2500)$ times greater than the Pb-Pb luminosity. On the other hand, Table II shows that the Pb-Pb cross sections are $\approx 30(20)$ times greater than the Ar-Ar(Ca-Ca) cross sections. Taking into account both luminosity and cross section behavior for each mode of the heavy ion LHC accelerator, one can realize that the total number of events in Ar-Ar(Ca-Ca) collisions is $\approx 8(125)$ times greater than in Pb-Pb collisions, which shows that Pb-Pb collisions is less indicated than Ar-Ar(Ca-Ca) collisions for photon-photon fusion processes with a typical center of mass energy of $\mathcal{O}(100)$ GeV. Therefore, the Pb-Pb mode will not be considered from this point on in our analysis.

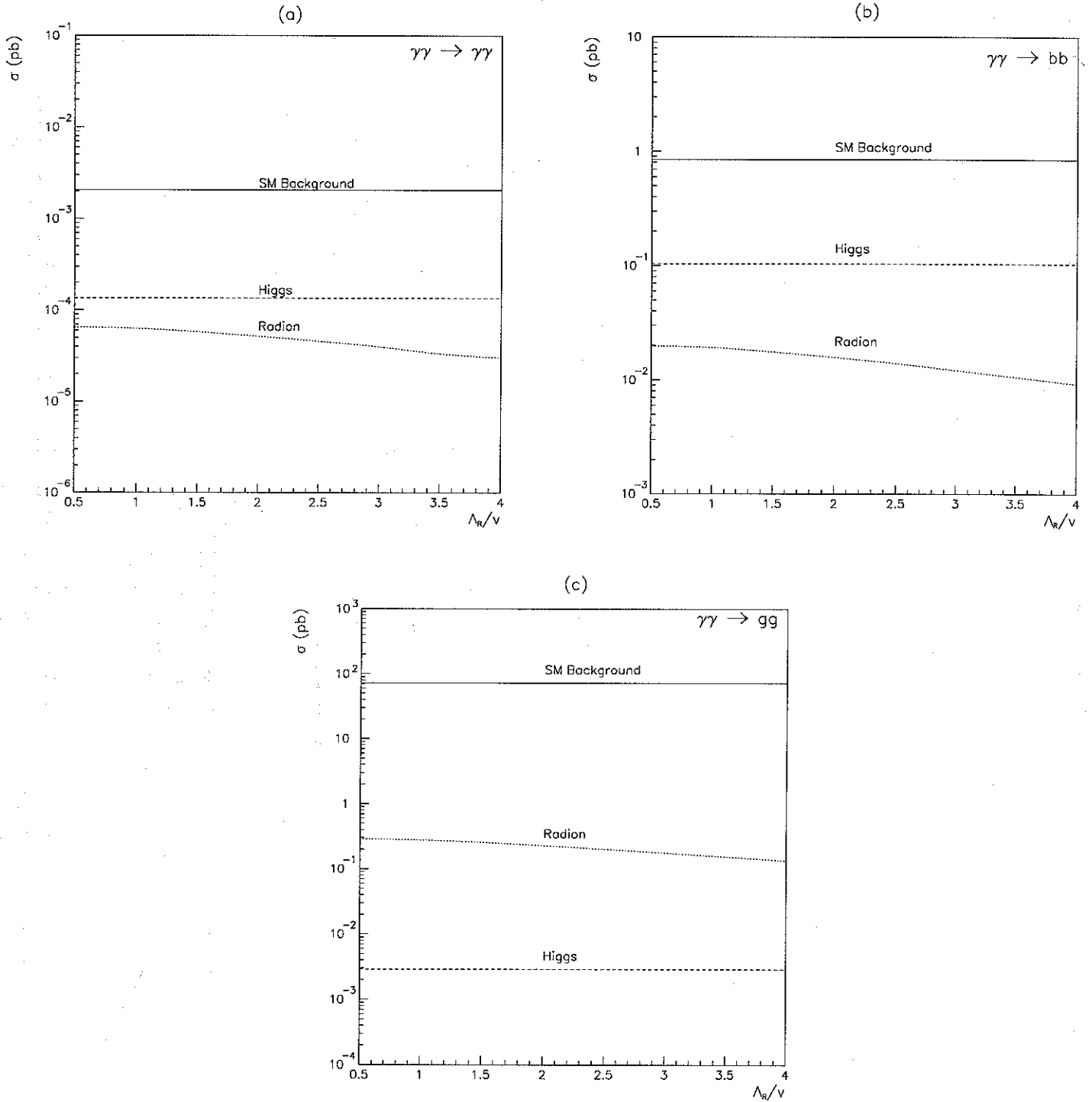


FIG. 4. Cross sections for the processes (a) $\gamma\gamma \rightarrow \gamma\gamma$, (b) $\gamma\gamma \rightarrow b\bar{b}$, and (c) $\gamma\gamma \rightarrow g\bar{g}$ in terms of the ratio of the vev's of the Radion (Λ_R) and the Higgs (v) fields. The mass of the Higgs and/or Radion is equal to 115 GeV and the set of cuts given by Equations (11) and (12) was applied. The full line corresponds to the SM background discussed in the text while the dashed (dotted) line corresponds to the Higgs (Radion) contribution.